Response to Reviewers
Manuscript: ACP-2017-842
Manuscript title: Investigating biomass burning aerosol morphology using a laser imaging nephelometer

The discussion below includes the complete text from the reviewer (bold), along with our responses to the specific comments and the corresponding changes (additions in italics, deletions struck through) made to the revised manuscript. All line numbers refer to the original manuscript.

Response to Reviewer #2 Comments:

This is a very interesting manuscript that describes the performance of a fairly novel polar Nephelometer used of the characterization of fresh biomass burning aerosols and their morphology. This is a generally well-written manuscript but it will need major revisions due to the lack of fractal analysis of SEM images (comments 11, 12) and the selective use of literature values (comments 7, 9, 12). However, it is appropriate for ACP and should be published after the following comments are taken into account.

We are grateful for the reviewer's careful consideration of the manuscript and appreciate their feedback. We have attempted to address his/her concerns and make the recommended revisions, as seen below.

1. P. 4 LiNeph: As this commercial polar nephelometer has not previously been described in the literature, a more detailed description would be desirable with more information on choice of wavelengths, beam dump, flow rates, curvature of beam image, etc. being of interest

The two wavelengths were chosen with the hope of seeing more evidence of absorption by brown carbon particles in the phase functions measured at 375 nm compared to those measured at 405 nm. Unfortunately, as absorption predominantly affects the backscatter, where the signal is relatively low, we were unable to observe these effects under these experimental conditions. In the future, we may try to do so by increasing the laser power (which would saturate the CCD at forward scatter angles) to have better signal-to-noise in the backscatter region. To address the question, we have added the following to the first paragraph of the Experimental section:

P.4 L.6: "…120 mW respectively. *These wavelengths were selected under the hypothesis that increased absorption by brown carbon particles at 375 nm compared 405 nm may be observable in the measured phase functions, however we were unable to observe this under the experimental conditions.* The output beams…"

We clarify the curvature of the beam in the Figure 2 caption as follows:

P.21 L.5: "~~The laser axis is curved due to the alignment with respect to the wide-angle lens.~~ *The blue dashed line shows the center of the laser beam; the slight curvature arises from the wide-angle lens being slightly off-center relative to the laser path.*"

The flow rates are given in Section 2.3, since this is somewhat dependent on the type of experiment.

2. P. 4 Image Processing: This section would benefit from quantification and examples for background spectra, wall scattering, etc.

We deepened discussion of the image processing approach with the following text and figure in the Supplementary. Note that the Supplementary figures have been renumbered to follow the sections of the main manuscript.

"Figure S2 depicts the relative contribution of different signals to the raw measurements. The data have all been summed across each angle bin. The raw data (black line) represent a single measurement of the total aerosol population during Fire A (see Section 4.1). The non-particle contributions are shown in colors and stacked. The Rayleigh scattering and helium correction have been scaled for laser power during the measurement, and the Rayleigh scattering has also been corrected for pressure. We note that a much higher laser power is used when measuring only Rayleigh scattering for calibration measurements. The dark background is predominantly accounted for by the voltage across the CCD; the standard deviation across the pixel array and variation for different acquisition times (100 ms compared to 10 s) accounts for < 5% of this signal level. The dark background appears to contribute substantially to the signal here because we have summed the signal across all pixels, including those not exposed to scattering from the laser beam (see Figure 2 in the main manuscript)."
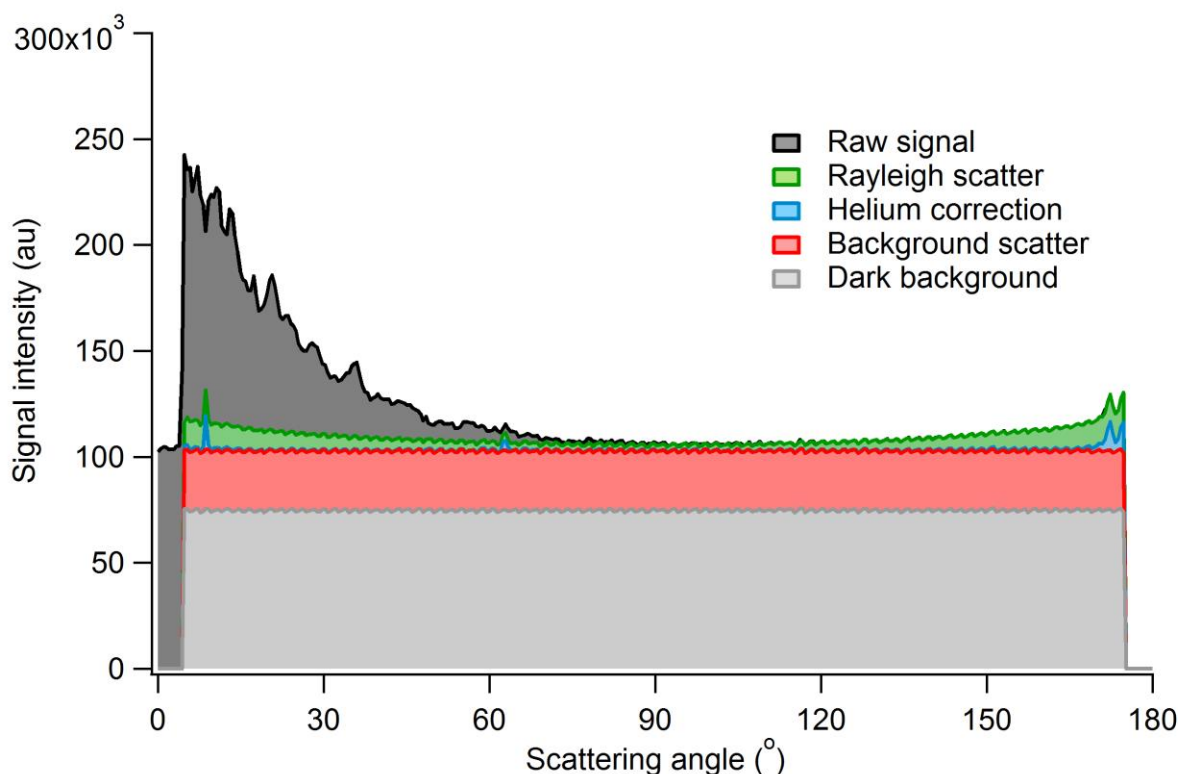

Figure S2: Contribution of various sources of signal to a single measurement of scattering of the total aerosol population (bypass channel) during Fire A. The black line indicates the raw signal summed across all pixels for each angle bin. The coloured lines show the corrections applied, and are stacked in the following order: dark background (grey), background scatter (likely caused by temperature variations of the CCD and multiple scatter from the walls), helium correction (direct wall scatter), and Rayleigh contribution. The dark background is dominated by the signal associated with the voltage across the CCD; read-out and single-shot thermal noise together account for <5%. The Rayleigh and helium corrections have been corrected for laser power, and the Rayleigh contribution has also been corrected for pressure. The integrated scatter from the aerosol particles was measured to be 88.3 Mm^{-1} in the instrument corresponding to 4741 Mm^{-1} in the original sample after accounting for dilution.

3. P.5, L.2: replace "aerosol-only" with "particle-only" as "aerosol" is defined as colloid of particles in air or other gases; i.e., aerosol includes the gaseous component.

Done.

4. P.4, L.12: "was found to be linear"; please quantify and show an example.

The following image and text have been added to the Supplementary and referenced in the main manuscript:

"Figure S3 shows a sample pixel-to-angle calibration curve for the 405 nm laser determined by comparing the pixel associated with the measured maxima and minima with the angles of the phase function maxima and minima predicted by Mie theory for monodisperse PSLs with diameters of 520, 600, and 700 nm."
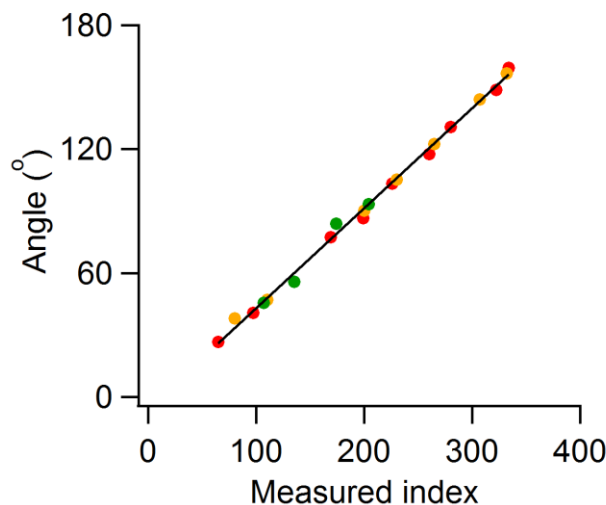

Figure S3: Pixel-to-angle calibration plot for 405 nm showing angles (calculated using Mie theory) versus measured indices for maxima and minima appearing in phase functions for monodisperse PSL: 520 nm (green), 600nm (orange), and 700 nm (red). The fit, including all sizes, has a slope of 0.484, intercept of -5.45, and R² value of 0.997.

5. P. 7, L.8 and elsewhere "fractal-like particles; and P. 8, L. 4 and elsewhere "fractal aerosols". Please decide if you want to call these particles "fractal-like" or "fractal" and use this consistently. Personally, I prefer "fractal-like" as the agglomerates are not purely fractal; the fractal nature breaks down below a certain length scale (monomer size).

We thank the reviewer for the suggestions. We have harmonized the text to use "fractal-like" when discussing particles and "fractal" when referring specifically to theoretical models.

6. P.7,L. 18: "and Abs(2ka(m-1)) << 1 with wavenumber (k=2pi) and a equal to the monomer radius." Why not just use the definition of the size parameter x for the monomer and replace with "and Abs (x(m-1)) << 1, where x is the monomer size parameter."?

We have made the following changes:

P.7 L.18: "… and ~~$|2ka(m-1)| \ll 1$ with wavenumber ($k = \frac{2\pi}{\lambda}$) and a equal to the monomer radius~~ $|2x_P(m-1)| \ll 1$ *with x_p equal to the size parameter of the monomer*."

7. P.8, L.4-6: "While fractal aerosols produced from fossil fuel combustion have been studied extensively, only one systematic measurement of the fractal parameterization of fresh biomass burning combustion products has been undertaken. Gwaze et al. (2006) measured k=2.77 and D=1.85 for biomass burning aerosol, although the authors note that 1.85 is a lower limit on Df."

What about the systematic analysis of fractal characteristics of particles emitted from the combustion of different biomass fuels given by Chakrabarty et al. (2006). Please cite and compare with Gwaze et al. (2006).

We thank the reviewer for pointing out this paper. We have incorporated this study into our discussion in Sections 3.1 and 4.3.

P.8 L.4-23: "While fractal aerosols produced from fossil fuel combustion have been studied extensively, ~~only one~~ *few* systematic measurement*s* of the fractal parameterization of fresh biomass burning combustion products *have* ~~has~~ been undertaken. *Chakrabarty et al. (2006) reported k_o values from 2.05 – 2.90 and D_f values in the range of 1.67 – 1.83 for various biomass fuels.* Gwaze et al. (2006) measured $k_o = 2.77$ and $D_f = 1.85$ for biomass burning aerosol, although the authors note that 1.85 is a lower limit on D_f. ~~In this work, unless otherwise noted, k_o and D_f are taken from Gwaze et al. (2006) since it is likely the most representative case for these measurements of biomass burning aerosol.~~ *In this work, unless otherwise noted, k_o and D_f are taken from Chakrabarty et al. (2006) based on fuel type.* The scattering angle-dependent structure factor, which allows calculating a RDG phase function, was adopted from Sorensen et al. (Liu et al., 2013a; Sorensen et al., 1992; Yang and Köylü, 2005). *Details of the phase function calculations based on the RDG model can be found in Liu et al. (2013a) and Kandilian et al. (2015).*

We used measured size distributions … For RDG model calculations, the monomer diameter (2*a*) was assumed to be 50 nm, based on SEM images and in agreement with *past studies of biomass burning (Chakrabarty et al., 2006; Gwaze et al., 2006)* ~~with Gwaze et al. (2006)~~. A wavelength-independent refractive index for black carbon ($m = 1.95 + 0.8i$) was assumed (Bond and Bergstrom, 2006). ~~As mentioned, the values of D_f and k_o were taken to be 1.85 and 2.77, respectively, based on reported fractal-like aerosol measurements in the literature, particularly for biomass burning emissions.~~ *The values of D_f and k_o were taken from the literature for similar fuel types and are detailed below (Chakrabarty et al., 2006). While the phase functions modeled using RDG are sensitive to these values, as well as the monomer diameter, a comprehensive analysis of the full range of possible RDG parameterization is beyond the scope of this paper; rather, here we present an initial "best guess" of the RDG parameterization based on the limited literature on biomass burning-produced soot and SEM micrographs.* Spherical particles were assumed to be predominantly organic material, and a representative refractive index for humic-like substances was assumed at each wavelength ($m = 1.64 + 0.12i$ at 375 nm; $m = 1.64 + 0.11i$ at 405 nm) (Hoffer et al., 2005; Lang-Yona et al., 2009). *A comparison of Mie theory calculations for a range of refractive indices is available in the Supplementary.*"

P.10 L.29-P.11 L.4: "Figure 6 shows measured phase functions … readily form spherical particles and be well-represented by Mie theory. *A comparison of phase functions assuming different refractive indices and fractal parameterizations is available in the Supplementary.* In contrast, the phase function of the denuded products looks much more similar to the RDG fractal model prediction based on the *ponderosa pine parameterization ($k_o = 2.32; D_f = 1.69$) from Chakrabarty et al. (2006)* ~~biomass burning parameterization~~ (Figure 6(b)). This would suggest that the refractory material has a predominantly fractal-like morphology that is well described using this parameterization for fresh biomass burning emissions."

P.11 L.17-19, L.33: "… the total aerosol population (Figure 8(a)) shows good agreement with the RDG model, assuming the *parameterization for sage fuel ($k_o = 2.56; D_f = 1.79$) from Chakrabarty et al. (2006).* ~~($k_o = 2.77; D_f = 1.85$) from Gwaze et al. (2006) for biomass burning products.~~ The agreement is

less good for … indicating no significant restructuring in the thermodenuder. *Unfortunately, no samples from Fire B were collected for SEM analysis."*

8. P. 8, L. 17: "manufacturers specifications for a similar instrument". Which instrument is this (please specify) and how similar are these instruments? Is the angular range identical?

Since submitting the original manuscript, we found the manufacturer's specifications for the LAS (the instrument used here), and so have noted that the angular range comes directly from the specifications for this instrument.

9. P. 8, L. 21-23: "Spherical particles were assumed to be predominantly organic material, and a representative refractive index for humic-like substances was assumed at each wavelength (m = 1.64 + 0.12i at 375 nm; m = 1.64 + 0.11i at 405 nm) (Hoffer et al., 2005; Lang-Yona et al., 2009). " Why do you use refractive indices for humic-like substances when refractive indices for OC from biomass burning (with much smaller imaginary parts) are readily available (Chakrabarty et al., 2010) and much more appropriate? Please explain and compare results when using either refractive index.

We thank the reviewer for the comment. We agree with the reviewer that the HULIS refractive index values represent a relatively absorbing OC, compared to the some of the brown carbon (BrC) studies. Nonetheless, organic carbon (OC) from biomass burning does not have a clear definition, nor a refractive index that is agreed upon across the literature. OC could include both tar balls (defined operationally as a type of near-spherical atmospheric aerosol particle consisting of amorphous carbonaceous material, which have been found to exist in abundance in polluted continental air masses) and BrC. Previous studies have found a wide range of possible imaginary refractive indices for BrC (Kirchstetter et al., 2004; Lack et al., 2012; Alexander et al., 2008; Saleh et al., 2014). For example Kirchstetter et al. (2004) reports highly absorbing k values at 400 nm (0.112) for organic carbon from biomass smoke, whereas Lack et al. (2012) shows very low k values at 404 nm for biomass burning (0.007 ± 0.005). The refractive index for OC given in Chakrabarty et al. (2010) is for what they term "tar balls". Chakrabarty et al. (2010) indeed show that tarballs are relatively non-absorbing (m = 1.78 + 0.015i and m = 1.83 + 0.0076i at 405 nm for two types of duff fuels). However, the definition of tar balls is vague, and their chemical composition and degree of volatility vary across the literature. Other studies found tar balls from biomass burning, to be highly absorbing (e.g. Alexander et al. (2008) reported a refractive index of 1.67 – 0.27i at 550 nm). The absorption, as well as the definition, of tar balls in the literature is still not clear.

We believe that the HULIS refractive indices represent intermediate values for these type of aerosols. In an effort towards completeness, we have added a comparison of phase functions for different refractive indices (Mie theory) and fractal parameterizations (RDG) to the Supplementary, and references to the figure in Sections 3.1 and 4.3. This figure includes the two refractive indices given for tar balls produced by duff combustion in the Chakrabarty et al. (2010) paper, as well as a completely non-absorbing aerosol as a reference. It should be evident from this graph that the refractive index of the organic material does not strongly influence the shape of the phase function predicted for spherical particles.

"Figure S7 shows a comparison of phase functions modeled using two different fractal parameterizations (RDG model) and four different refractive indices for spherical particles (Mie theory). This plot corresponds to Figure 6(a) in the main manuscript. It is evident that the values used do not significantly alter the general shape of the phase functions, with the RDG model always predicting much more strongly forward-scattering phase functions. Details of the parameterizations, including references, are noted in the caption."
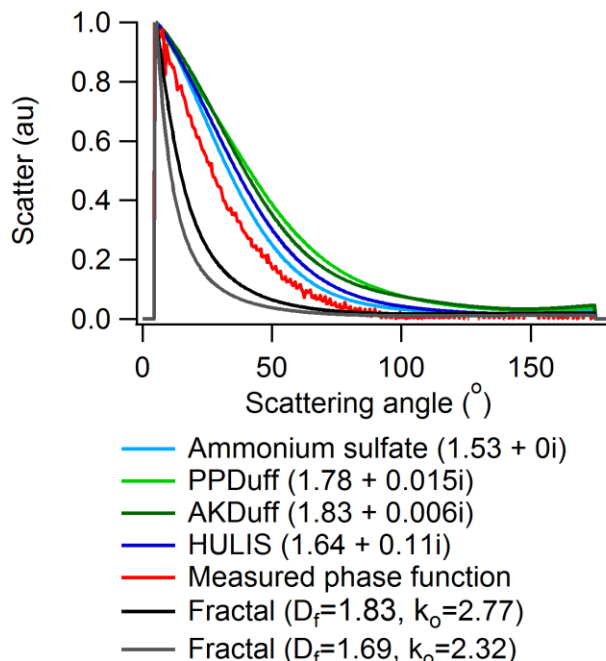
Figure S7: Intercomparison of measured and modelled phase functions using different parameterizations for Fire A (bypass channel) at 405 nm: measured (red); Mie theory using refractive index for ammonium sulfate (light blue) (Haynes, 2013), ponderosa pine duff (PPDuff; light green) (Chakrabarty et al., 2010), Alaskan duff (AKDuff; dark green) (Chakrabarty et al., 2010), and humic-like substances (dark blue) (Dinar et al., 2008); RDG theory using fractal parameterization for ponderosa pine (grey) (Chakrabarty et al., 2006) and beech (black) (Gwaze et al., 2006). All curves were normalized to unity at 5° scattering angle.

10. P.9, L.9: Replace "errors arising from the background signal is more systematic…" with "errors arising from the background signal are more systematic…".

The sentence has been fixed (P.9 L.9).

11. P11, L. 6-8: "This implication from the phase function measurements is further supported by SEM images (Figure 7), which show that the non-volatile (denuded) components are mostly fractal-like particles." A quantitative analysis of the SEM images for fractal-like parameters (dimension, pre-factor) is much needed to check applicability of literature values used for optical modeling.

While we would ideally like to incorporate a thorough quantitative fractal analysis to support our RDG parameterizations, unfortunately we are not able to do this for three reasons: (1) the samples were sputter coated with ~2 – 5 nm of Pt to prevent charging under the strong electron beam, preventing an accurate assessment of monomer overlap; (2) we did not perform a comprehensive study on whether the deposition onto the silicon substrate caused any deformation of the agglomerates or how many contact points the agglomerates have with the substrate; and (3) there is evidence of agglomeration post-deposition (agglomerates >> impactor cut point) concentrated at the center of the impaction site making it difficult to accurately assess the original fractal properties. However, we appreciate that some fractal analysis is beneficial to supporting our parameterization of the RDG model. We have therefore modified the following discussion in Section 4.3:

P.11 L.4-11: "~~Given the value of the fractal dimension (D_f = 1.85) is close to the minimum diffusion-limited case (~1.75), we assume the agglomeration was (nearly) diffusion-limited, and no significant restructuring or collapse of the particles occurred in the chamber.~~ This implication from the phase function measurements is further supported by SEM images (Figure 7), which show that the non-volatile

(denuded) components are mostly fractal-like particles. *Using the SEM software, the average monomer diameter was measured for monomers clearly visible on the outer edges of the agglomerates; the average monomer diameter (excluding Pt coating) is 50 ± 10 nm. A simple box-counting fractal analysis was performed using image analysis software (ImageJ, (Image Processing and Analysis in Java), National Institutes of Health) on the fractal-like particles measured from Fire A (thermodended) to estimate the fractal dimension (Karperien, 2013). This algorithm calculates a fractal dimension (D_{fB}) based on the relationship between the length scale (ε) and number of boxes containing a portion of the fractal at each scale (N_ε) (Theiler, 1990):*

$$D_{fB} \approx \frac{log(N_\varepsilon)}{log(\epsilon)}. \qquad (2)$$

The fractal dimension retrieved (1.87 ± 0.06) likely represents an upper limit as the Pt coating on the particles will increase apparent overlap of monomers. Both the monomer size and fractal dimension (considering it is an upper limit) are in line with the literature values used for the RDG models based on previous studies of biomass burning particles (Chakrabarty et al., 2006; Gwaze et al., 2006). Due to the coating, we are not able to retrieve the fractal dimension and prefactor using other methods previously demonstrated for fractal-like aerosol particles (Brasil et al., 1999; Chakrabarty et al., 2006). Additionally, it is unclear whether any deformation of the fractal-like agglomerates occurred upon deposition to the silicon substrate. Interestingly, there also appear to be a small fraction of spherical particles in the SEM micrographs that could fall into the classification of "tar balls" – amorphous, non-volatile organic aerosol previously observed in biomass burning aerosol populations that survive thermal denuding (Adachi and Buseck, 2011; Chakrabarty et al., 2010; *China et al., 2013;* Hand et al., 2005; Pósfai et al., 2004)."

12. P.11, L.17-19: "The phase function measured for the total aerosol population (Figure 8(a)) shows good agreement with the RDG model, assuming the parameterization (k=2.77; D=1.85) from Gwaze et al. (2006) for biomass burning products." This needs to be compared with other literature values (Chakrabarty et al., 2006) and even better with SEM characterization of fractal-like parameters.

Please refer to Comments 7 and 11 above.

13. P.11, L. 32: "the measurements suggest". Specify which measurements.

We clarify by making the following changes:

P.11 L.32-33: "However, *the shape of the measured phase function is qualitatively in agreement with models assuming fractal dimensions of 1.75 – 1.79 (Figure 8(b)), suggesting* ~~the measurements suggest~~ that the fractal dimension does not change *and, consequently,* ~~or decreases slightly, indicating~~ no significant restructuring in the thermodenuder."

14. P.25, Fig. 6 and P.27, Fig. 8: The y-axis is labeled with "Scatter (au)", however the figure caption states "Phase functions are normalized to total scatter in spherical coordinates." Which one is true? Also what do you mean by "scatter"; I'm not familiar with this term (differential scattering cross-section?), please change or explain and give reference.

In the literature, phase functions are typically normalized either for the total integral over all solid angles equal to unity or forward scatter equal to unity. We understand that the former method (which was used in the original manuscript) may be somewhat confusing, and is also more sensitive to noise in the side-scattering region where the signal-to-noise-ratio is relatively small. Therefore, in the updated draft we have selected the second method of normalization. As is commonly done, we have used arbitrary units

(au) on the axis, however "scatter" informs the reader that the normalized signal is proportional to the total scatter (in units of, i.e. Mm⁻¹). The new figures, with updated captions, are shown here:

(a) Fire A: Bypass channel

(b) Fire A: Thermodenuded

— Measured phase function
— Model phase function - Mie (spherical)
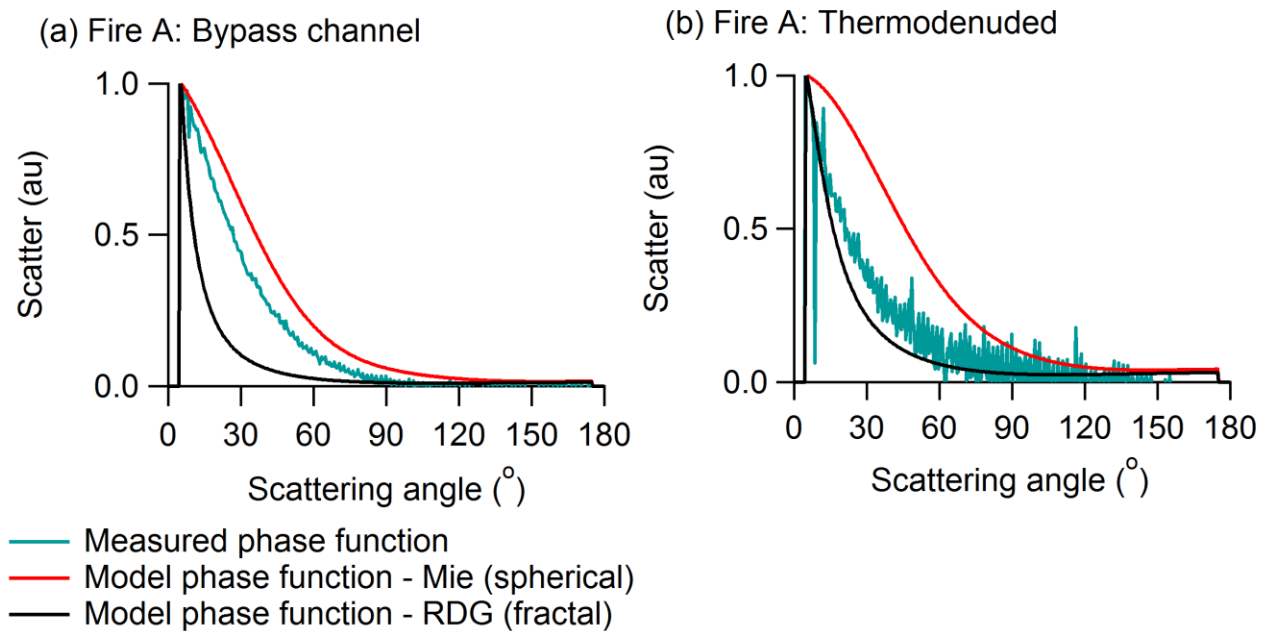— Model phase function - RDG (fractal)

Figure 1: Comparison of measured (blue) phase function at 405 nm to Mie theory model (red) and RDG model (black) for one cycle of sampling through bypass channel (a) and after the thermodenuder (b) for Fire A. *Phase functions are normalized to unity at 5° scattering angle. Mie theory calculations are based on HULIS refractive index (Dinar et al., 2008) and RDG calculations are based on ponderosa pine parameterization (Chakrabarty et al., 2006).*

(a) Fire B: Bypass channel

(b) Fire B: Thermodenuded

— Measured phase function
— Model phase function - Mie (spherical)
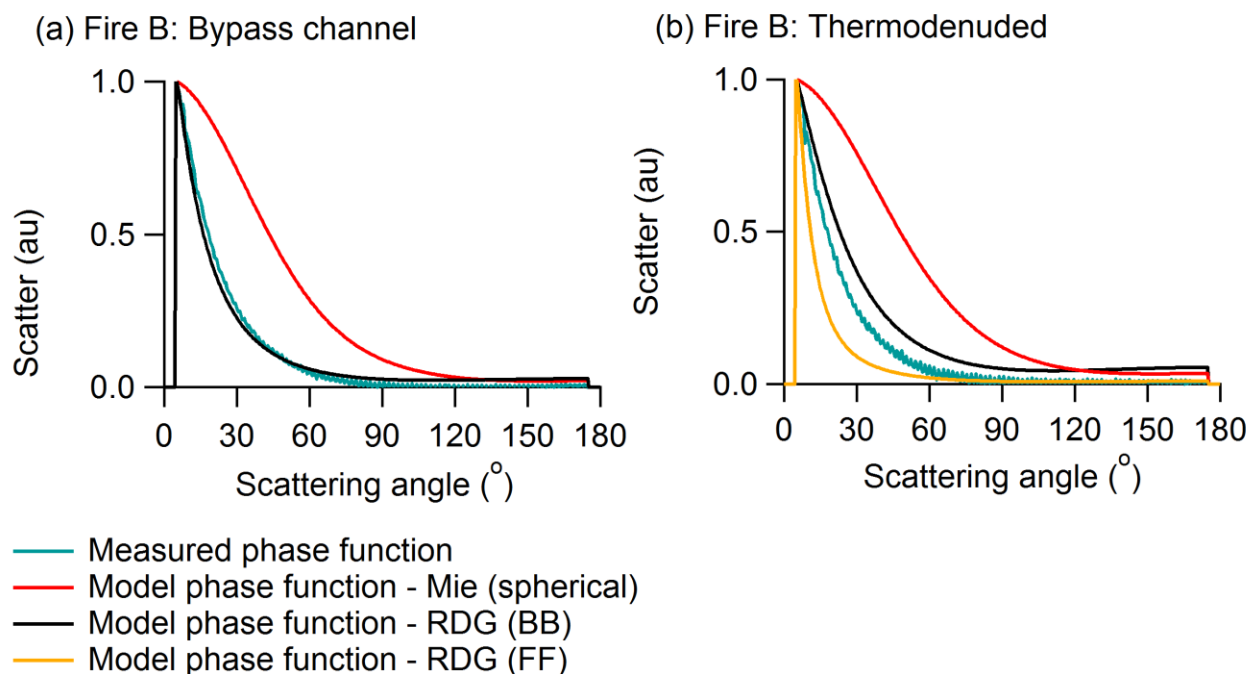— Model phase function - RDG (BB)
— Model phase function - RDG (FF)

Figure 2: Comparison of measured (blue) phase function at 405 nm to Mie theory model (red) and RDG models (black and orange) for one cycle of sampling through bypass channel (a) and after the thermodenuder (b) for Fire B. Two RDG parameterizations were compared: fossil fuel (FF; orange) and biomass burning (BB; black). *Phase functions are normalized to unity at 5° scattering angle. Mie theory calculations are based on HULIS refractive index (Dinar et al., 2008) and RDG calculations are based on sage fuel for biomass burning (BB) case (Chakrabarty et al., 2006) and laboratory combustion of fossil fuels (FF) (Sorensen, 2001).*

References

Chakrabarty, R. K., H. Moosmuller, M. A. Garro, W. P. Arnott, J. W. Walker, R. A. Susott, R. E. Babbitt, C. E. Wold, E. N. Lincoln, and W. M. Hao (2006). Emissions from the Laboratory Combustion of Wildland Fuels: Particle Morphology and Size. J. Geophys. Res. 111, doi:10.1029/2005JD006659.

Chakrabarty, R. K., H. Moosmuller, L.-W. A. Chen, K. Lewis, W. P. Arnott, C. Mazzoleni, M. K. Dubey, C. E. Wold, W. M. Hao, and S. M. Kreidenweis (2010). Brown Carbon in Tar Balls from Smoldering Biomass Combustion. Atmos. Chem. Phys., 10, 6363-6370.

Alexander, D. T. L., P. A. Crozier, and J. R. Anderson (2008). Brown carbon spheres in East Asian outflow and their optical properties. Science, 321, 833-836, doi:10.1126/science.1155296.

Saleh, R., M. Marks, J. Heo, P. J. Adams, N. M. Donahue, and A. L. Robinson (2014). Contribution of brown carbon and lensing to the direct radiative effect of carbonaceous aerosols from biomass and biofuel burning emissions. J. Geophys. Res.-Atmos., 120, 10285–10296, doi:10.1002/2015JD023697.

Kirchstetter, T. W., T. Novakov, and P. V. Hobbs (2004). Evidence hat the spectral dependence of light absorption by aerosols is affected by organic carbon. J. Geophys. Res., 109, D21208, doi:10.1029/2004JD004999.

Lack, D. A., J. M. Langridge, R. Bahreini, C. D. Cappa, A. M. Middlebrook, and J. P. Schwarz (2012). Brown carbon and internal mixing in biomass burning particles, P. Natl. Acad. Sci. USA, 109, 14802–14807, doi:10.1073/pnas.1206575109.